Dynamic Modelling and Simulation of Raw Meal Calcination for Isothermal Boundary Conditions

Lars-André Tokheim

Department of Process, Energy and Environmental Technology, University of South-Eastern Norway, Norway, {lars.a.tokheim@usn.no}@usn.no

Abstract

This article describes modelling and simulation of heating and calcination of raw meal particles. The purpose is to determine the time required to obtain a certain calcination degree for particles that are exposed to surroundings with a specified temperature. The impact of applying different reactor temperature values and different particle sizes is investigated. The aggregated calcination degree as a function of time is calculated for a typical raw meal with a specified particle size distribution and with different contents of $CaCO_3$ in different size classes. The developed model can be used as a basis for determining the required size of potential new calciner reactor types.

Keywords: Raw meal, Heat transfer, Calcination, Particle size distribution

1 Introduction

Raw meal is a finely ground mixture of solid materials used as the main feed in modern cement kilns. It usually contains 75-80 wt% calcium carbonate, $CaCO_3$. The rest is a mixture of mainly SiO_2, Al_2O_3 and Fe_2O_3 as well as some MgO, K_2O and Na_2O (Duda, 1985).

One of the key reactions occurring in the kiln system is calcination, in which the calcium carbonate decomposes into calcium oxide and carbon dioxide; $CaCO_3(s) \rightarrow CaO(s) + CO_2(g)$. This is an endothermic reaction that needs a temperature of around 900 °C to occur. After completion of calcination, further heating and partly melting of the solid material will take place. However, during the calcination process, which is the focus in this article, the other components in the meal (SiO_2, Al_2O_3, etc.) can be considered inert.

In a modern cement kiln system, the decarbonation reaction will be done in a separate calcination reactor. In the calciner, the particles are exposed to high temperature surroundings in the form of heat transfer surfaces, flames and hot combustion gases. Thermal radiation, convection and conduction all contribute in the heat transfer process.

Most calciners operate in the pneumatic conveying regime (Tokheim, 1999), i.e., the particles are vertically entrained by hot gases while being calcined. Such calciners typically have a gas residence time of 2-6 seconds, whereas the particle residence time may be several times longer due to internal recycling of particles inside the calciner. A long residence time is particularly important in cases where lumpy alternative fuels are to be utilized (Tokheim, 2006). The particle calcination process will benefit from a long residence time, meaning that a lower calcination temperature may be used.

Other types of calciners, operating in other regimes, for example bubbling fluidized bed (BFB) calciners (Samani et al., 2020) or drop tube calciners (Hills, 2017; Hodgson, 2018) may be of interest in cases where combustion gases are absent and the heat transfer is to be provided mainly through radiation from hot surfaces. Such reactors are of special relevance if the calcination process is to be electrified (Tokheim et al., 2019).

When designing new reactor types for the calcination process, it is necessary to understand the dynamic behavior of the calcining particles in order to size the reactor. The time required for calcination will largely depend on the particle size and the temperature in the reactor of interest. The size of the raw meal particles ranges from about 1 to 500 µm, and the median is typically 20-30 µm.

The purpose of this paper is to 1) develop a dynamic model of the heating and calcination of raw meal particles of difference size, and 2) combine this model with experimental data on particle size and chemical composition, in order to 3) determine the time required to obtain a certain calcination degree for an industrial raw meal exposed to a specified reactor temperature.

The contribution of this study is to provide a model that can be applied to industrial raw meal mixtures with a typical distribution of particle size and chemical composition. It will apply to systems with any CO_2 concentration in the calciner, including those operating with pure CO_2. The latter is relevant for electrically heated calciners.

2 Dynamic model of a particle being heated and calcined

In this section, the system is described, the mathematical model equations are explained, the discretized model equations are given and the model input values are listed.

2.1 System description

The heat transfer from the isothermal surroundings (e.g., a hot, temperature-controlled wall) to the particle mainly occurs through radiation. The supplied thermal energy is used for heating and calcining the particles.

The particle enters the calciner in a preheated state. When the particle is exposed to an environment with a higher temperature than the particle, it will be further heated. The environment for a particle is typically a gas surrounding the particle, a reactor wall constituting the boundary of the heat transfer domain, as well as other particles.

As the particle temperature increases, $CaCO_3$ will decompose; $CaCO_3(s) \rightarrow CaO(s) + CO_2(g)$. The higher the temperature, the faster the calcination. The calcination is endothermic, and the typical calcination temperature is around 900 °C, depending on the process conditions.

After a certain time, the calcination will be complete, and the particle is pure CaO (plus any inert components), as all CO_2 has been driven out. Any heat supplied after this, will result in further heating of the calcined particle, and the particle will gradually approach the temperature of the surroundings and hence reach a new constant level. However, in general, a calcination degree of 90-95 % is targeted, so the particle will in general not exceed the calcination temperature.

The process described above, is illustrated in Figure 1, where T_{calc} indicates the temperature at which conversion from $CaCO_3$ (blue) to CaO (red) starts.

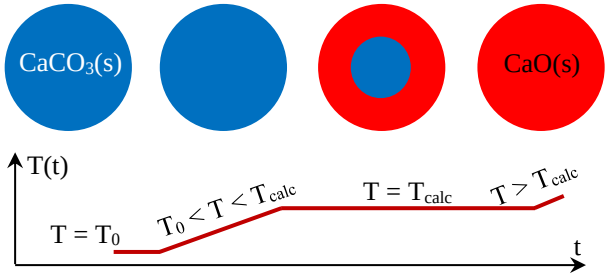

Figure 1. Heating and calcination of a $CaCO_3$ particle.

It should be noted that in an industrial process, the calcination degree (also called the degree of calcination, *DoC*) of the meal in the calciner should not exceed 90-95 %. This is because complete conversion will lead to a fast temperature increase in the reactor, and this may in turn cause unwanted sintering effects due to partial melt formation. In traditional calciner systems operating with fuel as the energy source, the *DoC* is kept in the range 90-95 % by adjusting the fuel feed rate to obtain a certain exit temperature, which by experience is found to give a suitable *DoC* value. The *DoC* value is checked regularly by sampling and laboratory analyses. A similar control concept can be applied for an electrified system, but then the electric power input is adjusted to comply with the temperature setpoint. Interlocks based on local wall temperatures should also be implemented to make sure overheating is avoided.

The uncalcined particle has a specified mass density and volume, i.e., a certain mass. During decarbonation, the particle mass will gradually decrease as CO2 is driven out. However, according to shrinking core model (Levenspiel, 1989), the volume of the particle is believed to stay approximately unchanged whereas the porosity will increase, meaning that the effective particle density will decrease.

There are many experimental studies on calcination kinetics available, typically involving the use of thermogravimetric analysis (TGA) to determine the mass loss as a function temperature and time (Ar et al., 2001; Garcia-Labiano et al., 2002; Valverde et al., 2015; Maya et al., 2018; Fedunik-Hoffman et al., 2019). Other types of furnaces are also used (Hu and Scaroni, 1996; Wang et al., 2007; Ghiasi et al., 2021). Many of these refer to Silcox et al. (1989), who developed a model to take into account decarbonation of $CaCO_3$ at the reactant-product interface, diffusion of CO_2 through the growing CaO layer and sintering of CaO. Some studies (for example, Hu and Scaroni,1996; Wang et al., 2005; Valverde et al., 2015) also apply scanning electron microscope (SEM) analyses to study how the structure of the limestone changes during the process. CaO sintering effects will reduce the porosity of the particles and thereby reduce the effective decompostion rate. The effect increases with increasing partial pressure of CO_2.

As pointed out above, different factors contribute to particle heat-up. However, in this study, only radiation heat transfer from the wall is considered. Convection and radiation heat transfer from the gas to the particle are neglected, as these contributions are believed to be quite small compared to the wall contribution, at least in the main energy-consuming phase, i.e., the calcination phase. Furthermore, radiation (and conduction) from other particles are neglected as all particles will likely have approximately the same temperature.

As the particles are small, spatial temperature gradients inside the particles are neglected, i.e., the particle temperature is assumed to depend on time only. For larger particles, the model should be used with caution.

Sintering effects, which may be significant for larger particles, are not included in this study, but may be implemented at a later stage.

In a real system, the particles will have different shapes. In this study, however, spherical particles are assumed. This makes it easy to calculate the surface area and the volume of the particle. The surface area is important because the heating is an area-specific process. The volume is required to calculate the initial mass of the particle.

2.2 Model equations

An energy balance of the particle may be given as in Equation 1, where E means energy [J], $\dot{E}$ means energy flow [W] and t is time [s]:

$$\dot{E}_{in} - \dot{E}_{out} + \dot{E}_{gen} = \frac{dE}{dt} \quad (1)$$

The inflow of energy, $\dot{E}_{in}$, can be described as the product of the heat flux, $q^{"}$ [W/m²], and the surface area of the particle, A_p [m²]:

$$\dot{E}_{in} = q^{"} A_p \quad (2)$$

Assuming that the particle is completely enclosed in large isothermal surroundings, the heat flux inflow can be expressed in terms of the radiation flux from the wall to the particle, which is a function of the wall temperature T_{wall} [K], the particle temperature (a variable input parameter), T [K], and the emissivity of the particle, ε [-]:

$$q^{"} = \varepsilon\sigma(T_{wall}^4 - T^4) \quad (3)$$

σ is the Stefan-Boltzmann constant, which has a value of $5.67 \cdot 10^{-8}$ W/(m²K⁴). The surface area is a function of the particle diameter, D_p [m] (another variable input parameter):

$$A_p = \pi D_p^2 \quad (4)$$

The outflow of energy will be zero as only heating is modelled in this study. This means that the term $\dot{E}_{out}$ in Equation 1 can be deleted.

The term $\dot{E}_{gen}$ in Equation 1 is a source term. In this case, the source term is a sink, i.e., it represents the endothermic reaction happening during calcination, and can be formulated as in equation 5, where r is the reaction rate [mol/(m²·s)], M_{CO_2} is the molecular mass of CO_2 [kg/mol] (constant) and ΔH_{calc} is the specific calcination enthalpy [J/kg] (another constant):

$$\dot{E}_{gen} = r A_p M_{CO_2} \Delta H_{calc} \quad (5)$$

The transient term (right-hand side) in Equation 1, can be re-written as:

$$\frac{dE}{dt} = \frac{d(mcT)}{dt} = Tc\frac{dm}{dt} + mc\frac{dT}{dt} \quad (6)$$

Here, c is the specific heat capacity of the particle [J/(kg·K)], whereas m is the particle mas [kg]. The specific heat capacity is a weak temperature function, but here it is taken as a constant. The temperature dependence is moderate, so this simplification should not give a big error if a representative mean temperature is applied.

The time derivative of the mass is included in Equation 6. By utilizing the mass balance of the particle, the term $\frac{dm}{dt}$ may be replaced by an algebraic expression:

$$\frac{dm}{dt} = -r A_p M_{CO_2} \quad (7)$$

By combining equations 1–6, the following first order differential equation is found:

$$\frac{dT}{dt} = \frac{A_p}{mc}\varepsilon\sigma(T_{wall}^4 - T^4) - \frac{A_p r M_{CO_2} \Delta H_{calc}}{mc} + \frac{T}{m} r A_p M_{CO_2} \quad (8)$$

The reaction rate in equation 8 may be expressed as a function of a rate constant, K_d [mol/(m²·s·Pa)], the equilibrium pressure of CO_2, $p_{CO_2,eq}$ [Pa], and the partial pressure of CO_2 in the gas surrounding the particle, p_{CO_2} [Pa] (which will be given by the process conditions):

$$r = K_d\left(p_{CO_2,eq} - p_{CO_2}\right) \quad (9)$$

The rate constant is a function of the temperature and two model constants, i.e. a frequency factor, A_d [mol/(m²·s·Pa)], an activation energy, E_d [J/mol], and the universal gas constant, R (8.314 J/(mol·K):

$$K_d = A_d e^{-\frac{E_d}{RT}} \quad (10)$$

The equilibrium pressure of CO_2 is also a function of the temperature and two model constants, A_{eq} [mol/(m²·s·Pa)] and E_{eq} [J/mol]:

$$p_{CO_2,eq} = A_{eq} e^{-\frac{E_{eq}}{RT}} \quad (11)$$

Equation 7 shows that the mass will drop if the reaction rate is positive, but will increase if the reaction rate is negative. The latter will occur if the equilibrium pressure of CO_2 is lower than the partial pressure – then carbonation ($CaO(s)+CO_2 \rightarrow CaCO_3(s)$) will happen instead of calcination. However, the mass may not have higher values than the initial (uncalcined) mass m_0 [kg] and not lower values than the minimum mass m_{min} [kg], which will be reached when all CO_2 has been expelled from the particle. These two constraints must be implemented in the model. The minimum mass may be calculated through equation 12, where M_{CaCO_3} is the molecular mass of calcium carbonate [kg/mol] and w_{CaCO_3} is the weight fraction of calcium carbonate:

$$m_{min} = m_0 \left(1 - \frac{M_{CO_2}}{M_{CaCO_3}} w_{CaCO_3}\right) \quad (12)$$

The initial mass may be calculated based on the particle volume, V_p [m³], and the initial particle density, $\rho_{p,0}$ [kg/m³]:

$$m_0 = \rho_{p,0} V_p \quad (13)$$

The particle volume is assumed constant, as a shrinking core model is assumed, and can be calculated as:

$$V_p = \frac{\pi}{6} D_p^3 \quad (14)$$

The particle density, ρ_p [kg/m³], is a function of the particle mass and the particle volume:

$$\rho_p = \frac{m}{V_p} \quad (15)$$

The degree of calcination, DoC, is a function of the initial particle mass, the minimum particle mass and the time-dependent particle mass:

$$DoC = \frac{m_0 - m}{m_0 - m_{min}} 100\% \quad (16)$$

Equation 8 shows that the temperature is impacted by three terms: i) the wall temperature term, which always gives a positive temperature contribution, ii) the calcination enthalpy term, which is negative during calcination (if $p_{CO_2,eq} > p_{CO_2}$), meaning that $r > 0$), but positive during carbonation if $p_{CO_2,eq} < p_{CO_2}$, meaning that $r < 0$); iii) the mass loss term, which gives a positive contribution during calcination, but negative during carbonation.

2.3 Discretized model equations

The first-order differential equations, Equation 7 and 8, can be discretized according to Euler's forward method (with index k):

$$\left(\frac{\Delta T}{\Delta t}\right)_k = \frac{A_p}{m_k c}\left(\varepsilon\sigma(T_{wall}^4 - T_k^4) - r_k M_{CO_2} \Delta H_{calc} + T_k r c M_{CO_2}\right) \quad (17)$$

$$T_{k+1} = T_k + \left(\frac{\Delta T}{\Delta t}\right)_k \quad (18)$$

$$\left(\frac{\Delta m}{\Delta t}\right)_k = -r_k A_p M_{CO_2} \quad (19)$$

$$m_{k+1} = m_k + \left(\frac{\Delta m}{\Delta t}\right)_k \quad (20)$$

In addition to equations 17 – 20, the algebraic equations given in equations 9 – 11 and 15 – 16 are solved for each time step, i.e., for each value of T_k.

2.4 Input values

Model constants, temperature dependent data and true constants are given in Table 1, whereas Table 2 gives input values for calculation of a base-case.

A particle size of 300 µm is within the range of the raw meal particle size distribution and is used here just as an example (other particle sizes are investigated later). A temperature of 658 °C was selected based on calculations carried out in a previous phase of the project (Tokheim et al., 2019), and this value is within the typical variation range of a modern cement kiln system. The $CaCO_3$ content of 77% is also a typical value for cement plants producing ordinary Portland cement. Finally, the partial pressure in current cement kiln systems is typically 0.2-0.3 atm in the calciner, but in this study, a value of 1 atm is used because 100 % CO_2 is the relevant case for calciners with indirect heat transfer from hot surfaces. In such cases, no combustion gases will be mixed with the CO_2 coming from the decarbonation.

Table 1. Values of model constants, thermophysical data and true constants used in the calcination model.

Symbol	Unit	Value	Remark
A_d	mol/(m²s·Pa)	$1.2 \cdot 10^{-5}$	Stanmore and Gilot (2005); Wang et al. (2007)
E_d/R	K	4 026	
A_{eq}	Pa	$4.19 \cdot 10^{12}$	
E_{eq}/R	K	20 474	
c	J/(kg K)	850	Approx. value
ε	-	0.9	Approx. value
$\rho_{p,0}$	kg/m³	2 700	Typical value
ΔH_{calc}	J/kg	$3.6 \cdot 10^6$	Typical value
M_{CO_2}	kg/mol	0.044	Constant
M_{CaCO_3}	kg/mol	0.100	Constant

Table 2. Base case input parameters in the model.

Symbol	Unit	Value
D_p	µm	300
T_{wall}	°C	1 050
T_0	°C	658
w_{CaCO_3}	wt%	77%
p_{CO_2}	atm	1
Δt	ms	20

The input variables are independent parameters that may take different values. Table 3 shows ranges to be applied in order to investigate how variations in some of these will affect the behavior of the particle.

The particle size variations reflects the variation in an industrial raw meal (cf. Section 1). A typical value for the wall temperature may be 1050°C. However, the maximum allowed value depends on the wall material, so lower and higher values are also investigated.

Table 3. Variation in input parameter values.

Symbol	Unit	Value
D_p	µm	1 – 300
T_{wall}	°C	950 – 1100

Table 4 shows that different size fractions in raw meal have different chemical compositions. The size classes were determined by manual sieving, and the weight fractions (w_i) in the raw meal as well as the $CaCO_3$ content in each size class were back calculated from XRF-measured values of CaO content in each size class.

This means that the fraction of material to calcine is different in different size classes, and this will influence the required calcination time.

Table 4. Content of $CaCO_3$ ($w_{CaCO3,i}$) in different size fractions (w_i) in raw meal.

$D_{p,i}$ [µm]	$w_{CaCO3,i}$	w_i [wt%]
16	80.5 %	54.9
48	78.9 %	26.1
77	73.0 %	9.4
108	64.0 %	4.4
163	54.6 %	3.6
600	48.4 %	1.7

3 Results and discussion

First, a base case is simulated, using the values given in Table 1 and 2. Next, selected input parameters are varied according to ranges given in Table 3. Finally, the calcination of a raw meal consisting of different particle sizes with different chemical composition is simulated for typical process conditions in an industrial calciner, as indicated in Table 4.

3.1 Base case

Figure 2 shows that the temperature first increases from the initial (inlet) temperature of 658 °C. This is due to the heat flux from the wall. As the temperature increases, the equilibrium pressure increases and reaches a stable plateau value after about 0.6 s. From then on, the temperature (and accordingly also the equilibrium pressure) stays constant at about 1005 °C until about 6.2 s. After this, the temperature rises to a new plateau, corresponding to the wall temperature, i.e. 1050 °C. The system has now reached the state of thermal equilibrium.

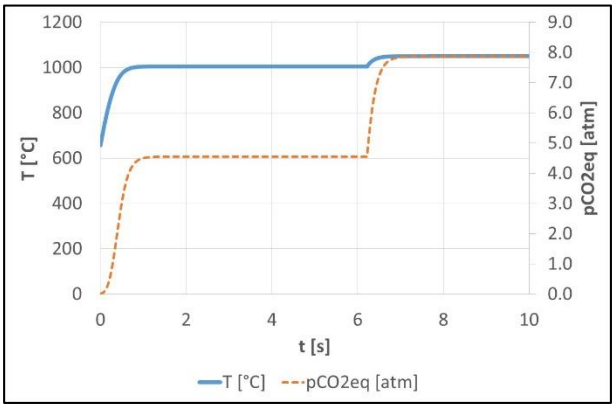

Figure 2. Temperature and equilibrium pressure as a function of time.

Figure 3 shows that the rate constant follows the same trend as the equilibrium pressure (cf. Figure 2), as the expressions given in equations 10 and 11 are both of a similar exponential nature. Moreover, the temperature gradient gradually drops and reaches a constant value, which abruptly increases for a short time when the calcination is complete. At equilibrium, it goes back to zero.

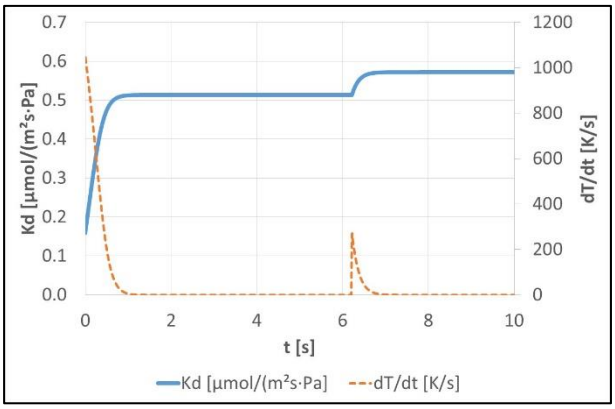

Figure 3. Rate constant and temperature gradient as a function of time.

Figure 4 shows that the particle mass is initially more or less constant for short period (about 0.1 s). This is because the reaction rate is low as the temperature is initially rather low. However, when the temperature and the reaction rate increase, the mass starts to drop. The mass reduction is linear in the period with a constant reaction rate. After about 6.2 s, the particle mass flattens out on a level corresponding to the minimum mass, as all CO_2 has been driven out of the particle, i.e. the calcination is complete. After this, the reaction rate drops to zero.

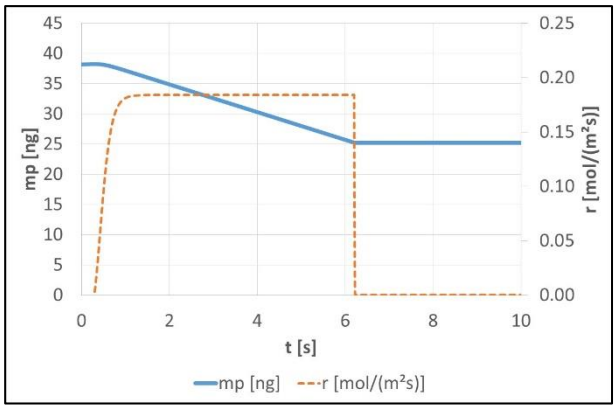

Figure 4. Particle mass and reaction rate as a function of time.

Figure 5 illustrates the co-variation of the temperature and the heat flux. Initially, the heat flux is extremely high, as there is a big difference between the wall temperature (1050 °C) and the particle temperature (658 °C). However, as the particle heats up, the flux drops quickly and reaches a constant level of about 20 kW/m² during the calcination period with a constant particle temperature. After completion of calcination, the particle temperature increases, which means that the driving force for the heat transfer drops, and eventually the flux reaches a zero value when the thermal equilibrium has been reached after about 7 s. However, as was mentioned in system description section, in a real system, the calcination process will be stopped before complete conversion occurs, so that high temperature levels and sintering effects are avoided.

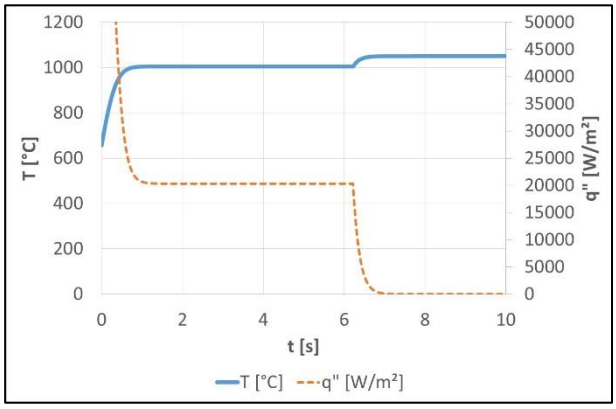

Figure 5. Heat flux and temperature as a function of time.

Figure 6 shows that the particle density drops from the initial level of 2700 kg/m³ to 1785 kg/m³ when the calcination is complete. After a very short period (about 0.6 s) with virtually no calcination, as the equilibrium pressure is lower than the partial pressure of CO_2, the calcination degree increases from 0 % to 100 %.

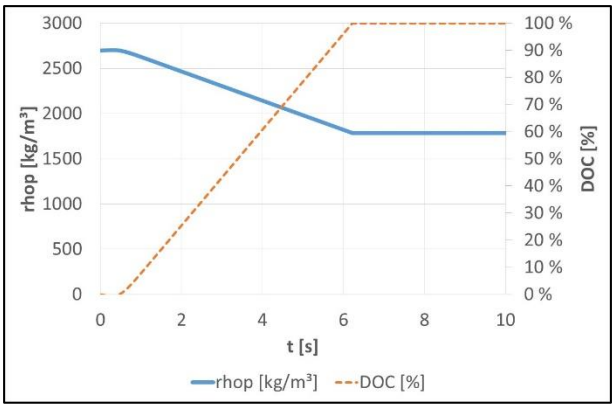

Figure 6. Particle density and calcination degree (*DoC*) as a function of time.

3.2 Variable particle size and temperature

Figure 7 shows that the reactor temperature and the particle size both have a big impact on the time required for complete calcination.

As an example, with a wall temperature of 1050 °C, a 100-µm particle needs 2.1 s to be completely calcined. If the wall temperature is 1100 °C, the required time is only 1.3 s. A very low wall temperature of 950 °C, on the other hand, increases the required conversion time to 9 s for this particle size. Similar differences are found for other particle sizes.

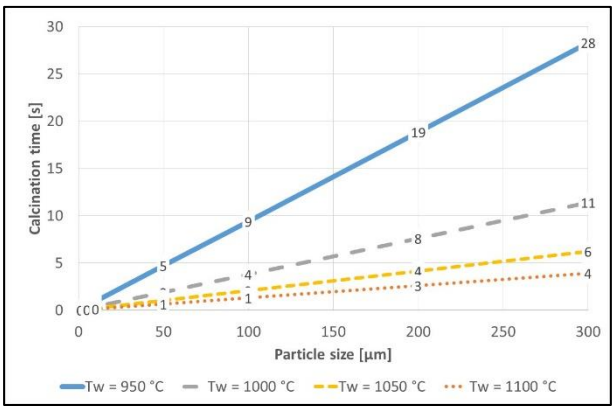

Figure 7. The impact of temperature and particle size on calcination time (T_0=658 °C, p_{CO_2}=1 atm, w_{CaCO_3}=1).

The calcination time is linearly dependent on the particle size. At a reactor temperature of 1050 °C, the calcination time increases from 2.1 s for a 100-µm particle to 6.3 s for a 300-µm particle.

3.3 Raw meal calcination

The calculated values of $CaCO_3$ content and weight fraction specified in Table 4 are used in the model to calculate the aggregated degree of calcination of the calcined meal at different residence times in the calciner.

The results are shown in Figure 8. The DoC values (calcination degree) seem to fit well with typical values in industrial calciners, in which 90-95 % conversion typically takes a few seconds (Tokheim, 1999).

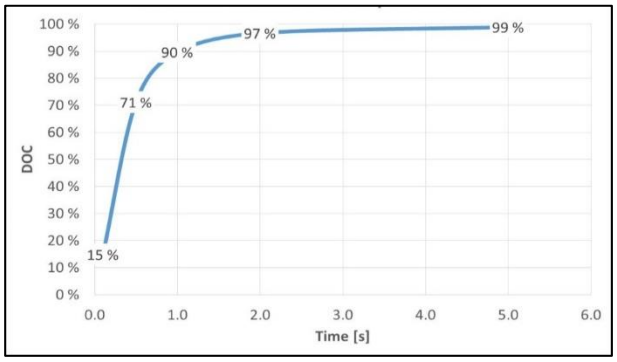

Figure 8. Raw meal calcination time (T_0=658 °C, p_{CO_2}=1 atm, T_{wall}=1050 °C, composition and particle size as given in Table 4).

4 Conclusion

The particle size and the reactor temperature are key variables controlling the calcination time for raw meal particles. A typical raw meal will be completely calcined in about 5 s when exposed to isothermal surroundings at 1050 °C. At lower temperatures, the calcination time will increase – and vice versa.

The model can be used as a basis for determining the required size of a potential new calcination reactor type, as different reactor types will operate at different temperatures. Developing a new reactor type is of particular interest in electrification of the calcination process, a concept that is currently being investigated aiming at a significant reduction in CO_2 emissions from cement plants employing electrified calcination.

Acknowledgements

This study was carried out as part of the research project "Combined calcination and CO_2 capture in cement clinker production by use of CO_2-neutral electrical energy – Phase 2". Gassnova and Norcem are greatly acknowledged for funding this project. Many thanks to Christoffer Moen, laboratory manager at Norcem, for reading and giving useful comments to the article.

References

Irfan Ar and Gülsen Dogu. Calcination Kinetics of High Purity Limestones. *Chemical Engineering Journal*, 83:131–137, 2001.

Walter H. Duda. *Cement Data Book Volume 1, 3rd edition*. Bauverlag GmbH, 1985.

Larissa Fedunik-Hofman, Alicia Bayon, and Scott W. Donne. Comparative Kinetic Analysis of $CaCO_3$/CaO Reaction System for Energy Storage and Carbon Capture. *Applied Sciences*, 9:4601, 2019. doi.org/10.3390/app9214601.

Vanessa Fierro, Juan Adánez, and Francisco García-Labiano. Effect of Pore Geometry on the Sintering of Ca-based Sorbents During Calcination at High Temperatures. *Fuel*, 83: 1733–1742, 2004. doi:10.1016/j.fuel.2004.03.011

Francisco García-Labiano, Alberto Abad, Luis F. de Diego, Pilar Gayán, and Juan Adánez. Calcination of Calcium-based Sorbents at Pressure in a Broad Range of CO_2 concentrations. *Chemical Engineering Science*, 57:2381–2393, 2002.

Meisam Ghiasi, Mahmoud Abdollahy, and Mohammadreza Khalesi. Investigating the Kinetics, Mechanism, and Activation Energy of Limestone Calcination Using Isothermal Analysis Methods. *Mining, Metallurgy & Exploration*, 38:129–140, 2021. doi.org/10.1007/s42461-020-00300-y.

Thomas P. Hills, Mark Sceats, Daniel Rennie, and Paul Fennella. LEILAC: Low Cost CO_2 Capture for the Cement and Lime Industries. *Energy Procedia*, 114:6166–6170, 2017. doi: 10.1016/j.egypro.2017.03.1753.

Phil Hodgson, Mark Sceats, Adam Vincent, Daniel Rennie, Paul Fennell, and Thomas Hills. Direct Separation Calcination Technology for Carbon Capture: Demonstrating a Low Cost Solution for the Lime and Cement Industries in the LEILAC Project. *14th International Conference on Greenhouse Gas Control Technologies (GHGT-14)*, 21st–25th October, Melbourne, Australia, 2018.

Naiyi Hu and Alan W. Scaroni. Calcination of Pulverized Limestone Particles Under Furnace Injection Conditions. *Fuel*, 75(2):177–186, 1996.

Octave Levenspiel, *The Chemical Reactor Omnibook*. OSU Book Stores, Oregon, USA, 1989.

Nastaran A. Samani, Chameera K. Jayarathna, and Lars-André Tokheim. Fluidized Bed Calcination of Cement Raw Meal: Laboratory Experiments and CPFD Simulations. *Linköping Electronic Conference Proceedings*, (61st SIMS conference, September 22–24), 399–406, 2020. doi.org/10.3384/ecp20176407.

Juan C. Maya , Farid Chejne, Carlos A. Gómez, and Suresh K. Bhatia. Effect of the CaO Sintering on the Calcination Rate of $CaCO_3$ Under Atmospheres Containing CO_2. *AIChE Journal - Reaction Engineering, Kinetics And Catalysis*, 64(10):3638–3648, 2018. doi.org/10.1002/aic.16326.

Geoffrey D. Silcox, John C. Kramlich, and David W. Pershing. A Mathematical Model for the Flash Calcination of Dispersed $CaCO_3$ and $Ca(OH)_2$ Particles. *Ind. Eng. Chem. Res.*, 28:155–160, 1989. doi:10.1016/j.fuproc.2005.01.023

Brian R. Stanmore and Patrick Gilot. Review – Calcination and Carbonation of Limestone During Thermal Cycling for CO_2 Sequestration. *Fuel Processing Technology*, 86:1707–1743, 2005.

Lars-André Tokheim. *The Impact of Staged Combustion On the Operation of a Precalciner Cement Kiln*, PhD dissertation, NTNU/TUC, 1999.

Lars-André Tokheim. Kiln System Modification for Increased Utilization of Alternative Fuels at Norcem Brevik, *Cement International*, 4:1–8, 2006.

Lars-André Tokheim, Anette Mathisen, Lars E. Øi, Chameera Jayarathna, Nils H. Eldrup, and Tor Gautestad.

Combined Calcination and CO_2 Capture in Cement Clinker Production by Use of Electrical Energy. *SINTEF Proceedings*, 4:101–109, 2019.

Jose M. Valverde, Pedro E. Sanchez-Jimenez, and Luis A. Perez-Maqueda, Limestone Calcination Nearby Equilibrium: Kinetics, CaO Crystal Structure, Sintering and Reactivity. *The Journal of Physical Chemistry*, 119:1623–1641, 2015. doi.org/10.1021/jp508745u

Yin Wang, Shiying Lin and, Yoshizo Suzuki. Study of Limestone Calcination with CO_2 Capture: Decomposition Behavior in a CO_2 Atmosphere. *Energy & Fuels*, 21:3317–3321, 2007. doi.org/10.1021/ef700318c.